CrossMark

Combined *TP53* mutation/3p loss correlates with decreased radiosensitivity and increased matrix-metalloproteinase activity in head and neck carcinoma

Sharat C. Raju [a], Samantha J. Hauff [a], Aaron J. Lemieux [a], Ryan K. Orosco [a], Andrew M. Gross [b], Linda T. Nguyen [a], Elamprakash Savariar [c], William Moss [a], Michael Whitney [c], Ezra E. Cohen [d], Scott M. Lippman [d], Roger Y. Tsien [c,e], Trey Ideker [b,f], Sunil J. Advani [g], Quyen T. Nguyen [a,c,d,*]

[a] Division of Head and Neck Surgery, University of California, San Diego, CA, USA
[b] Bioinfomatics and Systems Biology, University of California, San Diego, CA, USA
[c] Department of Pharmacology, University of California, San Diego, CA, USA
[d] Moores Cancer Center, San Diego, CA, USA
[e] Howard Hughes Medical Institute, San Diego, CA, USA
[f] Division of Medical Genetics, University of California, San Diego, CA, USA
[g] Department of Radiation Medicine and Applied Sciences, University of California, San Diego, CA, USA

ARTICLE INFO

SUMMARY

Objective: Patients with head and neck squamous cell carcinoma (HNSCC) containing *TP53* mutation and 3p deletion ("double-hit") have poorer prognosis compared to patients with either event alone ("single-hit"). The etiology for worse clinical outcomes in patients with "double-hit" cancers is unclear. We compared radiosensity of cell lines containing both *TP53* mutations and deletion of Fragile Histidine Triad (*FHIT*, the gene most commonly associated with 3p deletion) to "single-hit" lines with only *TP53* mutation. We compared radiosensitivity in a "single-hit" cell line with *TP53* mutation converted to "double-hit" using RNA interference targeting *FHIT*. Finally, we compared matrixmetalloproteinase-2/9 (MMP-2/9) activity, a previously-established biomarker for tumor aggressiveness, in xenograft tumors derived from these cell lines.

Materials/methods: *TP53* mutation and *FHIT* deletion profiles of HNSCC lines were established using Cancer Cell Line Encyclopedia (CCLE). We used RNA-interference to convert a "single-hit" cell line (SCC4) to "double-hit". Cultured cells were examined for radiosensitivity and cisplatin sensitivity. MMP-2/9 activity was evaluated in "double-hit" versus "single-hit" tumors using ratiometric activatable cell-penetrating peptide (RACPP) in tongue ($n = 17$) and flank xenografts ($n = 4$).

Results: Radiotherapy caused greater double-stranded DNA breaks in "single-hit" vs naturally occurring and engineered "double-hit" cells. In-vivo, "double-hit" xenografts demonstrated higher MMP-2/9 activity compared to "single-hit" xenografts ($p < 0.01$). There was no difference in cisplatin sensitivity between the cell lines.

Conclusions: *TP53* mutation combined with *FHIT* deletion correlates with decreased radiosensitivity in HNC cell lines. Xenograft from "double-hit" cells exhibit increased MMP-2/9 activity. These findings may in part account for the worse clinical outcome seen in patients with HNSCC "double-hit" tumors.

© 2015 Elsevier Ltd. All rights reserved.

Introduction

Head and neck squamous cell carcinoma (HNSCC) is a source of significant morbidity and mortality worldwide [1]. Well-established risk factors for HNSCC include tobacco, alcohol, and human papilloma virus (HPV) [1]. Current staging and clinical management HNSCC patients are based on anatomical location and size [2]. If patients undergo surgical excision, management decisions are guided by presence or absence of bony invasion, lymph-node metastasis, or lymph-node extracapsular spread. Patients with locally advanced disease are treated with multimodality therapy including chemotherapy, radiotherapy and surgery.

* Corresponding author at: University of California San Diego, 9500 Gilman Drive La Jolla, CA 92093, USA. Tel.: +1 858 822 3965; fax: +1 858 534 5270.
E-mail address: q1nguyen@ucsd.edu (Q.T. Nguyen).

Many prevalent malignancies such as breast, colon, lung, or prostate cancer have diagnostic assays based on genomic profiling, HER-2 and estrogen receptor expression, or ALK, EGFR and KRAS mutation. HPV has recently been identified as being responsible for the increasing incidence of oropharyngeal SCC (OPSCC) [3,4], and HPV positive (HPV+) tumor status is currently the strongest prognostic factor for these patients [4,5]. However, there are currently no widely adopted prognostic assays for HPV-negative (HPV−) HNSCC.

We previously analyzed The Cancer Genomic Atlas (TCGA), which contains the largest collection of patient HNSCC tumor specimens [6]. In HPV–tumors, reduced survival outcomes associated with tumor protein p53 (TP53) mutation occur only in combination with loss of chromosome 3p [6]. In these patients, median survival decreased from >5 years for TP53 mutations to only 1.7 years for both mutational events ("double-hit") [6]. These findings are independent of clinical stage and replicated in an independent HNSCC cohort [6]. In HPV + tumors, we believe E6-mediated inactivation of TP53 also acts in synergy with 3p deletion to produce poor survival outcomes [6].

Our prior analysis of the TCGA demonstrated that of the genes on the 3p chromosome, FHIT, a known tumor suppressor gene involved in aerodigestive cancer, best correlates with 3p status [6]. The FHIT gene is located on a chromosomal fragile site, and loss of the 3p arm is most commonly mediated by chromosome breakage at this site [7]. Thus, 3p deletion is commonly associated with decreased FHIT protein expression or reduced copy number at the 3p.14.2 FHIT locus [7]. Given these findings, our analysis in this study uses FHIT copy number as representative of 3p status and thus a proxy for "single hit" (TP53 only) vs "double hit" (TP53 and FHIT deletion) in HNSCC cell lines. It has also been shown that FHIT and p53 status are linked in development of lung cancer, although little is known about the molecular nature of this interaction [8]. Here, we analyze data from the TCGA to examine whether TP53 and 3p status are linked in HNSCC patients.

The etiology for worse clinical outcomes in TCGA patients with "double-hit" cancers is unclear. Potential explanations include greater resistance to radiation monotherapy or more aggressive tumor biology in cancers with the "double hit." We do not anticipate a difference in cisplatin sensitivity given its lack of efficacy as monotherapy in clinical practice. To examine these hypotheses, we obtained four human tongue squamous cell carcinoma cell lines from American Type Culture Collection (ATCC). We utilized the Cancer Cell Line Encyclopedia (CCLE) to examine differences in their TP53 mutational and FHIT copy number status, corresponding with the prognostic markers identified in the TCGA.

To compare radiosensitivity in vitro, we utilized a comet-tail assay to measure each cell line's ability to repair ionizing radiation-induced double-stranded deoxyribonucleotide (DNA) damage. FHIT knockout has been previously associated with increased activation of the ATR/CHK1 pathway and stronger cell-cycle checkpoint responses, resulting in greater cellular repair in response to ionizing radiation [9]. We would thus expect reduced radiation-induced DNA damage in "double-hit" lines with FHIT deletion compared to "single-hit" lines with intact FHIT.

We also examined the aggressiveness of "single-hit" versus "double-hit" cell lines by comparing their respective matrix-metalloproteinase (MMP) activity levels. MMP expression has previously been associated with tumor aggressiveness and patient prognosis in head and neck cancer [15–19]. Absolute levels of MMP2/9 have been used to differentiate between benign papillomas and carcinoma of the larynx [15]. Increased MMP2/9 expression has been correlated with higher cancer grade [16] and reduced survival in HNSCC [17,18]. In tongue SCC, increased MMP2/9 expression directly correlates with incidence of lymph node metastases [19]. Recently, our own work has demonstrated that MMP over-expres-

sion in HPV + tumors predicts poorer survival [14]. Additionally, HPV–tumors, which have a more aggressive phenotype compared to their HPV + counterparts, also express higher levels of MMP [14]. We compared MMP activity in our cell lines using previously described ratiometric activatable cell-penetrating peptides (RACPP) [10–12]. The RACPP relies on tumor-associated MMP2/9 to cleave an intervening linker, resulting in increased Cy5/Cy7 fluorescent signal ratio, and has previously been used for margin detection during surgery [12–14].

Methods

Cell culture

HPV-lines SCC-4 SCC-15, and SCC-25 (ATCC) were maintained in Dulbecco's modified Eagle's medium with nutrient mixture F-12 (DMEM/F-12) containing 10% fetal bovine serum (FBS), supplemented with 400 ng/mL of hydrocortisone. HPV-HNSCC line CAL-27 (ATCC) was maintained in DMEM containing 10% FBS. Cells were incubated at 37 °C in 5% CO_2.

Analysis of the Cancer Cell Line Encyclopedia (CCLE)

The CCLE (Broad Cancer Institute) is the largest publicly-available compilation of cell line data, including information regarding gene expression, chromosomal copy number, and mutational status for 33 known tumor suppressor and oncogenes. We extracted data regarding normalized FHIT copy number, reported as $\log_2$(copy number)/2, and TP53 mutational status for all cell lines utilized in the study.

In-vitro radiosensitivity assay

Neutral comet assay was used to measure ionizing radiation (IR) induced DNA double-strand breaks. Cells were grown to 70% confluence, irradiated with IR, harvested 15 min post IR, suspended in agarose gel and lysed per assay directions (Trevigen). Samples underwent electrophoresis under neutral conditions and were then stained with Sybr Green. Comet tails were counted in multiple fields (>50 cells per sample) and analyzed using CometScore (TriTek Corp). To minimize bias, slides were analyzed in a blinded manner to treatment. 10–15 fields per slide were imaged randomly to achieve a fair representation.

In-vitro cisplatin sensitivity assay

Cells were plated in 96-well plates over a 24-h period. Starting cell counts were 2.5 K per well for SCC cell lines and 1.25 K per well for CAL-27. The starting counts were determined based on previous cell growth curves to prevent cell overgrowth and contact inhibition during the assay. Varying concentrations of cisplatin mixed in media (0–100 μM) were added to the cells. Each combination of cell line and cisplatin concentration was replicated in quintuplicates. Cells were incubated for another 72 h before undergoing a MTT proliferation assay to evaluate growth. Cell growth in cisplatin-exposed wells was recorded as a percentage of non-exposed wells. Initial IC_{50} and kill curves were generated using SigmaPlot.

RNA interference

The 293T producer cell line was transfected with small hairpin ribonucleic acid (shRNA) expressing lentiviral constructs and packaging plasmid mix (System Biosciences) using X-tremeGENE (Roche, Indianapolis, IN). pGIPZ_FHIT lentiviral vectors (#113,859, #225,339, #267,106, #307,150, #307,152 and #307,153) were

obtained from GE Dharmacon (Lafayette, CO). Supernatants were collected 48 h after transfection, filtered using a 0.45-μm-pore-size nitrocellulose filter, and applied to SCC-4 cells. After 48 h, the cells were selected in puromycin (2 μg/ml) containing media. As a control, cells were infected with a lentivirus expressing scrambled control shRNA (pGIPZ non-silencing shRNAmir RHS 4346, Openbiosystems).

RNA was extracted using the RNeasy Mini kit (Qiagen). One step QRT-PCR was performed using Brilliant II SYBR Green Master Mix (Agilent Technologies) and a Stratagene™ Mx3000p Q-RT-PCR system (Stratagene, La Jolla, CA). Primers used for detecting FHIT expression were (pair#1 AATACCTGCCTGCTTAGACC and CGAAG-GACAGTTCTGTTTTG and pair#2 TCTGTAAAGGTCCGTAGTGC and CGAAGGACAGTTCTGTTTTG). Protein Phosphatase-2 (PP2A) was used for internal control. Gene knockdown was calculated using the ΔΔ-Ct method.

RACPP peptide synthesis

RACPP was synthesized as previously described [15]. RACPP contains a Cy5 fluorophore attached to a poly-cationic moiety and a Cy7 fluorophore connected to a neutralizing poly-anionic arm. The fluorophores are bridged via a linker that is cleavable by MMP-2 and MMP-9. Following MMP cleavage of RACPP, FRET between Cy5 and Cy7 is disrupted and the polycationic portion conjugated to Cy5 becomes trapped within nearby tissue, thus dramatically increasing the Cy5/Cy7 ratio.

Cell culture and mouse tumor xenografts

Tongue xenografts: nu/nu mice (aged 3–6 months) were injected with cells ($\sim10^6$ for CAL-27, $\sim5 \times 10^6$ for SCC-4, SCC-15, SCC-25) into the anterior tongue (20 μL total volume) to generate orthotopic xenografts.

Flank xenografts: nu/nu mice were injected with cells under the skin overlying the flank ($\sim10^6$ for CAL-27, $\sim5 \times 10^6$ for SCC-4, 100 μL volume). Two SCC-4 and two CAL-27 injections were performed for each mouse.

The number of injected cells reflects different rates of tumor formation between the cell lines. We wanted to establish consistency in timing and size of tumor formation among all cell lines.

In-vivo imaging with RACPP

Mice with tumor size ≥ 4–5 mm or weight loss ≥ 20% were anesthetized with isoflurane and injected intravenously with RACPP (0.4 nmol RACPP/g body weight in 100 μL of nanopure water). Two hours following RACPP injection, mice were re-anesthetized (100 mg/kg ketamine and 5 mg/kg midalozam) for imaging.

For tongue tumors, soft tissues of the neck were surgically exposed and imaged (Maestro, Cambridge Research and Instrumentation, Woburn, MA) to obtain a background Cy5/Cy7 ratio. The mouse was also imaged supine with the tongue exposed. After whole-mouse imaging, the mouse was euthanized by isoflurane overdose and cervical dislocation. The entirety of the tongue from base to tip was excised and imaged separately (Maestro, CRI).

For flank tumors, the masses were carefully dissected from the overlying skin. Mice were then imaged with the flank skin removed and the underlying tumors exposed (Maestro, CRI). Cy5/Cy7 ratios from surrounding muscle were used as background to generate normalized Cy5/Cy7 ratios for flank tumors.

Multi-spectral imaging involved exciting Cy5 at 620 ± 10 nm followed by use of a tunable LCD emission filter to perform stepwise emission measurements from 640 to 840 nm. Numerator (Cy5) and denominator (Cy7) images were generated by integrating spectral images over pre-defined wavelengths (660–720 nm for Cy5 and 760–830 nm for Cy7). Ratio images were created and color-encoded as hue (blue–red scale) using custom software. Monochromatic Cy5 and Cy7 images were also generated for processing in Image J.

Image processing and ratio calculations

Monochromatic Cy5 and Cy7 images were extracted from multispectral cube images using custom software, as described above. The "Image Calculator" function was utilized on Image J to divide the Cy5 image by the Cy7 image, generating a new image where the Cy5/Cy7 ratio was encoded as pixel intensity. Ratios were averaged from regions of histologically-confirmed tumor. Mean tumor Cy5/Cy7 ratios were then normalized to Cy5/Cy7 ratios of background tissue.

Histologic processing and pathologic examination

Following imaging, tongue and flank tissues were embedded in cryopreservative, frozen in liquid nitrogen, and stored at −80 °C. 5-μM sections were fixed in formalin and stained with hematoxylin and eosin (H&E). The samples were evaluated by a pathologist blinded to experimental conditions.

Statistics

For multiple groups, statistical analysis was performed with one-way ANOVA. Individual groups were compared with an independent sample student t-test. Paired data was compared using a two-tailed paired sample t-test. Statistical significance was set at a p-value of less than 0.05.

Results

Cell line mutational data from the CCLE

We examined the CCLE for TP53 mutational status and FHIT (3p.14.2) copy number of ATCC tongue SCC cell lines utilized in this study (Table 1). All cell lines (SCC-4, SCC-15, SCC-25, CAL-27) were represented in the CCLE.

Normalized FHIT copy numbers ($\log_2$CopyNumber/2) were −0.507, −6.34, −5.48, and −5.92 for SCC-4, SCC-15, SCC-25, and CAL-27 respectively (Table 1). These copy numbers suggest homozygous loss of FHIT ($FHIT^{-/-}$) for SCC-15, SCC-25, and Cal-27, and FHIT heterozygosity ($FHIT^{+/-}$) for SCC-4. The TP53 gene was mutated in all cell lines. SCC-4 contains a missense mutation (G→A) on nucleotide 7578479 of chromosome 17p, SCC-15 harbors a splice-site mutation (C→T) on nucleotide 7578176, SCC-25 has a frame-shift deletion event starting on nucleotide 7578222, and CAL-27 contains a missense mutation (T→A) on nucleotide 7578271.

In summary, the mutational profiles of the SCC-15, SCC-25, and CAL-27 cell lines correlate with the "double-hit" patients seen in our prior TCGA analysis, due to the presence of both FHIT loss and TP53 mutation. In contrast, the SCC-4 cell line harbors a TP53 mutation without loss of FHIT, thus reflecting a "single-hit" mutational profile.

Cell lines with combined FHIT deletion and TP53 mutation are more resistant to ionizing radiation

The primary mode of cell death following conventional fraction doses of IR is mitotic catastrophe through IR induced lethal DNA double strand breaks. To investigate the hypothesis that cell lines

Table 1
Cancer cell line encyclopedia mutation data for HNSCC cell lines.

Cell line	TP53 mutational status	Normalized FHIT copy number	Overall mutational status
SCC4	Missense mutation	−0.507	Mut TP53
SCC 15	Splice site mutation	−6.34	FHIT deletion Mut TP53
SCC 25	Frame-shift/deletion	−5.48	FHIT deletion Mut TP53
CAL 27	Missense mutation	−5.92	FHIT deletion Mut TP53

with the "double-hit" mutation–deletion profile are more resistant to radiotherapy, we performed a neutral comet-tail assay on all cell lines following treatment with 2-Gy of radiation. This dose of IR is clinically relevant as HNSCC patients treated with radiotherapy are treated with daily fractions of 2 Gy.

Using comet-tail length as an indicator of DNA double strand breaks, we found increased sensitivity to irradiation in the "single-hit" SCC-4 cell line compared to the "double-hit" cell lines, SCC-15, SCC-25, and CAL-27. Upon exposure to 2 Gy, the SCC-4 cell line demonstrated a longer comet tail length of 133.96 ± 6.83 versus 64.90 ± 7.27 in SCC-15 ($p < 10^{-9}$), 33.31 ± 7.13 in SCC-25 ($p < 10^{-9}$), and 54.79 ± 4.18 ($p < 10^{-9}$) in CAL-27 (Fig. 1B). In
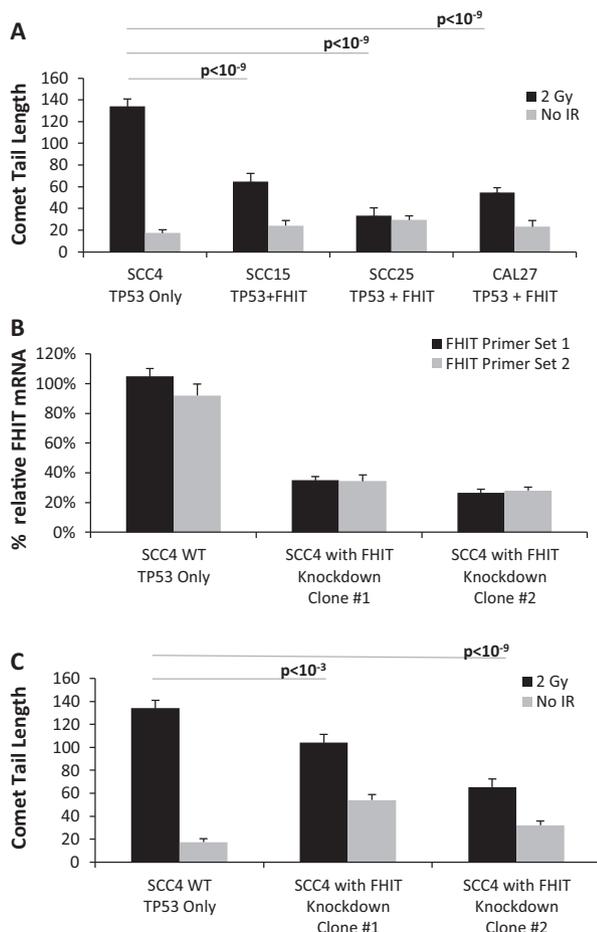

Fig. 1. HNSCC cell lines with both TP53 mutation and FHIT deletion are more radio-resistant compared to a HNSCC cell line containing only TP53 mutation. Knockdown of FHIT in a HNSCC cell line originally containing only a TP53 mutation increases radioresistance. (A) When exposed to 2 Gy ionizing radiation (black bars), the SCC-4 cell line, containing only a TP53 mutation, demonstrates greater double-stranded DNA breaks, as measured by comet-tail assay, compared to SCC-15, SCC-25, and CAL-27 cell lines, which contain both TP53 mutation and FHIT deletion. (B) Using RNA interference, we decreased FHIT expression by almost 80% in SCC-4 cell line. (C) When exposed to 2 Gy ionizing radiation, the wild-type SCC-4 cell line, containing only TP53 mutation, demonstrated greater double-stranded DNA breaks compared to clones containing TP53 mutation with FHIT knockdown.

non-irradiated cells, there was no difference in comet-tail length between the 4 HNSCC cell lines (SCC-4: 17.39 ± 3.12, SCC-15: 24.04 ± 4.80, SCC-25: 29.28 ± 3.76, CAL-27: 23.15 ± 5.57), indicating that the double-stranded breaks were appropriately radiation dependent (Fig. 1A).

Knockdown of FHIT in cell lines with TP53 mutation induces resistance to radiation treatment

To further investigate whether "double-hit" mutated cell lines are more radioresistant than "single-hit" cell lines, we knock down FHIT expression in our SCC-4 cell line using RNA interference (RNAi). The wild-type (WT) SCC-4 cell line only possesses a TP53 mutation, thus down-regulating FHIT expression effectively approximates a "double-hit" cell line. We confirmed adequate knockdown of FHIT expression in RNAi SCC-4 clones using Quantitative Real-Time Polymerase Chain Reaction (QPCR) with two sets of primers. WT SCC-4 demonstrated relative FHIT expression, compared to standard, of $104.77\% \pm 5.28\%$ and $91.95\% \pm 7.59$, using primer sets 1 and 2 respectively. We obtained 6 clones of RNAi producing FHIT expression ranging from 26% to 80% of wild type. Clones 1 and 2 were selected as they showed the lowest FHIT expression levels: Clone #1 of RNAi SCC-4 demonstrated FHIT expression levels of $34.92\% \pm 2.59\%$ and $34.42\% \pm 4.06\%$. Clone #2 FHIT expression levels were $26.59\% \pm 2.30\%$ and $28.02\% \pm 2.45\%$ (Fig. 1B).

We compared radiosensitivity in WT SCC-4 with RNAi SCC-4 clones using the previously described comet tail assay. We found increased sensitivity to irradiation in WT "single-hit" SCC-4 cell lines compared to RNAi "double-hit" SCC-4 clones. Upon exposure to 2 Gy, WT SCC-4 demonstrated a longer comet tail length of 133.96 ± 6.83 versus 103.93 ± 4.90 in Clone #1 of RNAi SCC-4 and 65.34 ± 4.76 in Clone #2 of RNAi SCC-4 (Fig. 1C).

Cell lines have similar sensitivity to cisplatin mono-treatment regardless of FHIT/TP53 status

We next investigated the hypothesis that all cell lines were similarly resistant to chemotherapy by performing a cisplatin sensitivity assay. Cells were incubated in varying concentrations of cisplatin for 72 h. Cisplatin inhibitory concentration (IC_{50}) values were measured as $1.75 \mu M \pm 0.09$ for SCC-4, $1.63 \mu M \pm 0.29$ for SCC-15, $4.64 \mu M \pm 0.28$ for SCC-25, and $2.39 \mu M \pm 0.41$ for CAL-27 (Supp Fig. 1), representing no biologically significant difference in cisplatin sensitivity between cell lines.

Xenografts with combined FHIT deletion and TP53 mutation have increased MMP2/9 activity

Using our MMP2/9 cleavable RACPP probe, we evaluated *in vivo* MMP-2/9 activity of tumor xenografts derived from our cell lines. Cleavage of RACPP by tumor-associated MMP2/9 results in increased Cy5/Cy7 fluorescence ratio. We have previously used these xenografts to examine the role of RACPP in margin detection for HNSCC, but did not examine differences between "double-hit" and "single-hit" cell lines [14].
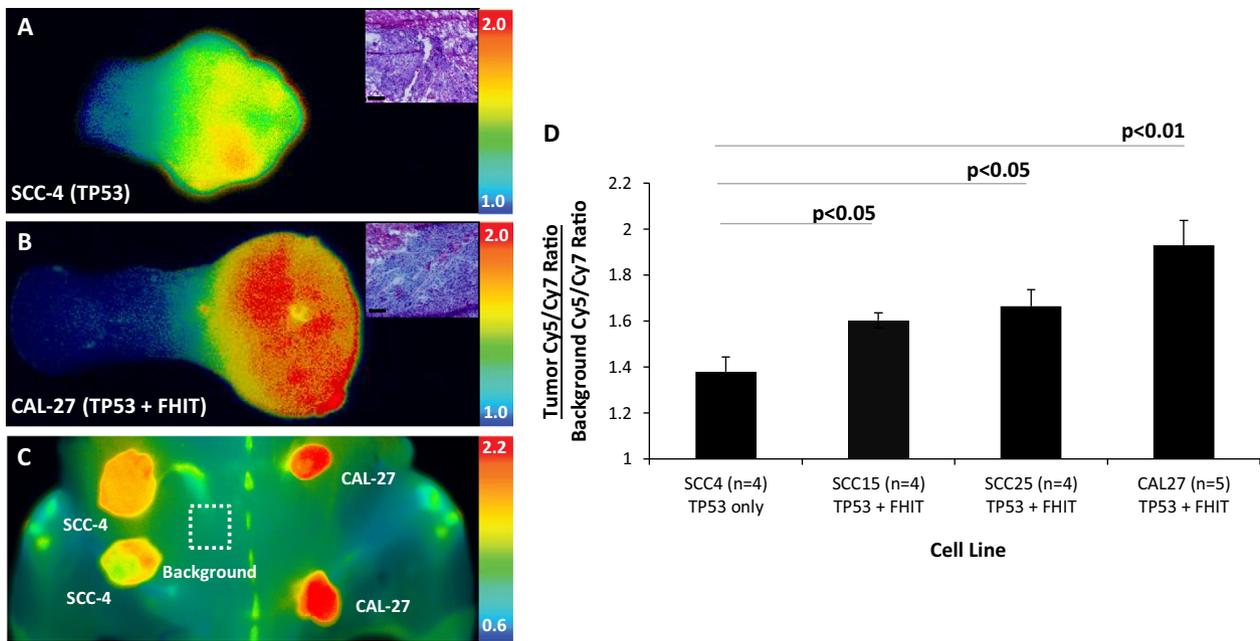
Fig. 2. Xenografts from HNSCC cell lines with both *TP53* mutation and *FHIT* deletion demonstrate higher MMP activity compared to those from cell lines with only *TP53* mutation. Legend: MMP-cleavable RACPP demonstrates lower fluorescent signal contrast in (A) histology-confirmed SCC-4 tongue xenografts, containing only a *TP53* mutation, compared to (B) CAL-27, containing both *TP53* mutation and *FHIT* deletion. (C) Greater MMP activity in CAL-27 flank xenografts compared to SCC-4 xenografts, when implanted in the same mouse. (D) Bar graph demonstrating higher MMP activity in xenografts from cell lines with both *TP53* mutation and *FHIT* deletion compared to xenografts from cell lines with only *TP53* mutation.

Following intravenous injection of RACPP, tumors were imaged in the living mouse as previously described. Following imaging, tumors were excised and confirmed histologically by a pathologist blinded to experimental conditions. Mean Cy5/Cy7 ratios, normalized to background were 1.38 ± 0.06 for SCC-4 (Fig. 2A, D), 1.93 ± 0.11 for CAL-27 tumors (Fig. 2B, D) and 1.66 ± 0.07 for SCC-25, 1.60 ± 0.03 for SCC-15 (Fig. 2D). Mouse xenografts derived from "double-hit" *TP53/FHIT* cell lines, including SCC-15, SCC-25, and CAL-27, demonstrated a higher normalized mean Cy5/Cy7 ratio compared to xenografts derived from the "single-hit" *TP53* SCC-4 cell line ($p < 0.05$ for SCC-25 and SCC-15 vs SCC-4, $p < 0.01$ for CAL-27 vs SCC-4, Fig. 2D). CAL-27 also demonstrated higher normalized mean Cy5/Cy7 ratios compared to SCC-25 and SCC-15 ($p < 0.05$ for each).

To reduce experimental variability produced by RACPP dosing and distribution, we employed a flank tumor model in which a given single mouse was injected with both SCC-4 and CAL-27 tumor cells, thus decreasing inter-animal variability in RACPP cleavage ($n = 4$ mice, 8 SCC4 tumors, 8 Cal-27 tumors). We found higher mean normalized Cy5/Cy7 ratios for "double-hit" CAL-27 flank tumors compared to "single-hit" SCC-4 flank tumors (2.05 ± 0.112 for CAL-27, 1.52 ± 0.037 for SCC-4, $p < 0.005$), consistent with the tongue xenograft data (Fig. 2C).

Discussion

Epithelial cancers of the head and neck remain a challenging disease to manage and outcome is among the worst of any cancers. Mortality remains high for most patients, and curative therapy can be quite morbid and impair survival quality of life. Targeted therapy to tumor specific biomarkers has long been an aim of head and neck cancer research; however, it has remained an elusive goal to-date. The utility of such identified biomarkers could be threefold: developing targeted cancer therapies, stratifying treatment aggressiveness, and improving prognostic capabilities. Identification of

HPV's role in the development of HNSCC has led to progress in the latter two of these goals, but little headway has been made for HPV-negative tumors.

We have previously found in HPV-HNSCC tumor specimens from TCGA that *TP53* mutation commonly occur in combination with loss of chromosome 3p [6]. In these patients, median survival decreased from >5 years for *TP53* mutations to only 1.7 years for both mutational events ("double-hit") [6]. In this study, we evaluated potential mechanistic etiologies that may account for this observation.

We compared radiosensitivity of "double-hit" HNSCC cell lines containing both *TP53* mutations and deletion of *FHIT* (as a proxy for 3p deletion) to "single-hit" lines with only *TP53* mutation. We also compared sensitivity to ionizing radiation in a "single-hit" cell line converted to "double-hit" using RNA interference. We found that the combined genomic events of *TP53* mutation and *FHIT* deletion correlate with decreased radiotherapy sensitivity in HNSCC cell lines. Increased resistance to radiotherapy could, in part, account for the poor clinical outcome of patients with the "double-hit" profile. This findings parallels prior studies demonstrating increased radioresistance in cells with *FHIT* knockout [9].

MMP2/9 mRNA expression has previously been correlated with increased HNSCC clinical aggressiveness [15–19]. We compared matrix-metalloproteinase-2/9 (MMP-2/9) activity between xenograft tumors derived from "double-hit" versus "single-hit" cell lines. We found that xenograft tumors from "double-hit" cell lines have increased MMP-2/9 activity compared to tumors from "single-hit" cell lines, which could also account, in part, for the poor clinical outcome of patients with the "double-hit" profile.

Cisplatin is rarely utilized as a mono-therapy and typically given as a radio-sensitizer. Additionally, all of our HNSCC cell lines contain *TP53* mutation- they only vary with respect to *FHIT* status. Previous studies have shown that cisplatin sensitivity is highly dependent on a functioning p53 protein. Mutation of *TP53* in all cell lines would wash-out any differences in terms of cisplatin sensitivity. Our findings support our original hypothesis that no

significant difference in cisplatin sensitivity exists between "single-hit" and "double-hit" cell lines.

Discovery of the "double-hit" phenomenon of 3p loss and *TP53* mutation offers the potential for improved management of HPV-HNSCC [6]. The *in vitro* and *in vivo* experiments described here, using "single hit" versus "double hit" cell lines, support our findings from the TCGA cohort. The combined genetic event of *FHIT* loss and *TP53* mutation in established HNSCC cell lines and xenografts confer resistance to radiotherapy and increased MMP2/9 activity. Whether the correlation between MMP-2/9 activity and the combined 3p-*TP53* events are causally linked or simply both markers of "bad actors" remains to be seen. In future studies, we hope to compare the effect of ionizing radiation on xenografts derived from "single hit" versus "double hit" cell lines.

These findings suggest a potential mechanistic etiology for the poor clinical outcome observed in patients with "double-hit" HPV-HNSCC tumors and may provide new molecular targets for treatment.

Conflict of Interest

Authors MW, RYT and QTN are scientific advisors to Avelas Biosciences which has licensed ACPP technology from UCSD.

Acknowledgements

Appendix A. Supplementary material

Supplementary data associated with this article can be found, in the online version, at http://dx.doi.org/10.1016/j.oraloncology.2015.01.014.

References

[1] Ferlay J, Shin HR, Bray F, Forman D, Mathers C, Parkin DM. Estimates of worldwide burden of cancer in 2008: GLOBOCAN 2008. Int J Cancer 2010;127(12):2893–917.

[2] Edge SB, Byrd DR, Compton CC, Fritz AG, Greene FL, Trotti A. AJCC cancer staging manual. Am Joint Comm Cancer 2010.

[3] Gillison ML. Human papillomavirus-associated head and neck cancer is a distinct epidemiologic, clinical, and molecular entity. Semin Oncol 2004;31(6):744–54.

[4] Benson E, Li R, Eisele D, Fakhry C. The clinical impact of HPV tumor status upon head and neck squamous cell carcinomas. Oral Oncol 2014;50(6):565–74.

[5] Chaturvedi AK. Epidemiology and clinical aspects of HPV in head and neck cancers. Head Neck Pathol 2012;6(suppl 1):S16–24.

[6] Gross AM, Orosco RK, Shen JP, et al. Multi-tiered genomic analysis of head and neck cancer ties TP53 mutation to 3p loss. Nat Genet 2014;46(9):939–43.

[7] Gollin SM. Cytogenetic alterations and their molecular genetic correlates in head and neck squamous cell carcinoma: a next generation window to the biology of disease. Genes Chromosom Cancer 2014;53(12):972–90.

[8] Andriani F, Roz E, Caserini R, et al. Inactivation of both FHIT and p53 cooperate in deregulating proliferation-related pathways in lung cancer. J Thorac Oncol 2012;7(4):631–42.

[9] Hu B, Han SY, Wang X, et al. Involvement of the FHIT gene in the ionizing radiation-activated ATR/CHK1 pathway. J Cell Physiol 2005;202(2):518–23.

[10] Olson ES, Aguilera TA, Jiang T, et al. In vivo characterization of activatable cell penetrating peptides for targeting protease activity in cancer. Integr Biol (Camb) 2009;1(5–6):382–93.

[11] Aguilera TA, Olson ES, Timmers MM, Jiang T, Tsien RY. Systemic in vivo distribution of activatable cell penetrating peptides is superior to that of cell penetrating peptides. Integr Biol (Camb) 2009;1(5–6):371–81.

[12] Savariar EN, Felsen CN, Nashi N, et al. Real-time in vivo molecular detection of primary tumors and metastases with ratiometric activatable cell-penetrating peptides. Cancer Res 2013;73(2):855–64.

[13] Nguyen QT, Olson ES, Aguilera TA, et al. Surgery with molecular fluorescence imaging using activatable cell-penetrating peptides decreases residual cancer and improves survival. Proc Natl Acad Sci USA 2010;107(9):4317–22.

[14] Hauff SJ, Raju SC, Orosco RK, et al. Matrix-metalloproteinases in head and neck carcinoma-cancer genome atlas analysis and fluorescence imaging in mice. Otolaryngol Head Neck Surg 2014;151(4):612–8.

[15] Uloza V, Liutkevičius V, Pangonytė D, Saferis V, Lesauskaitė V. Expression of matrix metalloproteinases (MMP-2 and MMP-9) in recurrent respiratory papillomas and laryngeal carcinoma: clinical and morphological parallels. Eur Arch Otorhinolaryngol 2011;268(6):871–8.

[16] Wittekindt C, Jovanovic N, Guntinas-lichius O. Expression of matrix metalloproteinase-9 (MMP-9) and blood vessel density in laryngeal squamous cell carcinomas. Acta Otolaryngol 2011;131(1):101–6.

[17] Liu WW, Zeng ZY, Wu QL, Hou JH, Chen YY. Overexpression of MMP-2 in laryngeal squamous cell carcinoma: a potential indicator for poor prognosis. Otolaryngol Head Neck Surg 2005;132(3):395–400.

[18] Mallis A, Teymoortash A, Mastronikolis NS, Werner JA, Papadas TA. MMP-2 expression in 102 patients with glottic laryngeal cancer. Eur Arch Otorhinolaryngol 2012;269(2):639–42.

[19] Zhou CX, Gao Y, Johnson NW, Gao J. Immunoexpression of matrix metalloproteinase-2 and matrix metalloproteinase-9 in the metastasis of squamous cell carcinoma of the human tongue. Aust Dent J 2010;55(4):385–9.